Article

Synthesis, Antimicrobial Study and Molecular Docking Simulation of 3,4-Dimethoxy-β-nitrostyrene Derivatives as Candidate of PTP1B Inhibitor

Salman Alfarisi [1], Mardi Santoso [2], Alfinda Novi Kristanti [1], and Ni Nyoman Tri Puspaningsih [1,3,*]

[1] Department of Chemistry, Faculty of Science and Technology, Universitas Airlangga, Kampus C-UNAIR, Mulyorejo, Surabaya 60115, Indonesia; salman.alfarisi-2017@fst.unair.ac.id; alfinda-n-k@fst.unair.ac.id

[2] Department of Chemistry, Faculty of Science and Data Analytics, Institut Teknologi Sepuluh Nopember, Kampus ITS, Sukolilo, Surabaya 60111, Indonesia; tsv09@yahoo.com

[3] Proteomic laboratory, Research Center for Bio-Molecule Engineering, Universitas Airlangga, Kampus C-UNAIR, Mulyorejo, Surabaya 60115, Indonesia

* Correspondence: ni-nyoman-t-p@fst.unair.ac.id; Tel.: +62-0811-345-2009

Abstract: A derivative series of 3,4-dimethoxy-β-nitrostyrene were synthesized and identified including new compound **6**. The effect of antimicrobial activity of 3,4-alkyloxy modification of β-nitrostyrene was investigated. A molecular docking was also performed to obtain information about their interactions with Protein Tyrosine Phosphatase 1B (PTP1B). PTP1B containing cysteine 215 and arginine 221 as essential active residues plays a key role in signaling pathways that regulate various cell functions of microorganisms, which also act as negative regulator in signaling pathways of insulin that are involved in type 2 diabetes and other metabolic diseases. Compound **5** and **6** were the most potent as fragment of PTP1B inhibitor based on molecular docking, but compound **5** was more effective against *Candida albicans*. These compounds interact with serine 216 and arginine 221 residues. However, further research is needed to investigate their potential medicinal use.

Keywords: 3,4-dimethoxy-β-nitrostyrene derivatives; antimicrobial agent; PTP1B, molecular docking

1. Introduction

The frequency of invasive and systemic fungal infections has increased dramatically according to disease severity and higher worldwide incidence. Unfortunately, only a few of the antifungal drugs which are currently available for the treatment of systemic mycoses are ideal in terms of antifungal spectrum, efficacy and safety [1,2].

Compounds containing a β-nitrostyrene fragment have been avowed as having bioactivity. In previous works, several β-nitrostyrene compounds have lately been examined as candidate of anticancer. The identified pharmacophore of their activity was the nitroethenyl side chain of the aromatic ring. The research of the antifungal and antibacterial activities of this frame of structures during the past decade is rather rare, eventhough the study in this field have been carried out since the 1940s. In many cases, the β-nitrostyrene structures were known to be stronger against gram-positive bacteria than other type of bacteria [3].

Park and Pei argued that β-nitrostyrene is a reversible tyrosine phosphatase inhibitor, thereby inhibiting and interfering protein tyrosine phosphatases (PTPs) that restrains cell signaling in microorganisms. Eukaryotic Tyrosine phosphorylation controls the normal cellular growth, cell-to-cell communication, cell differentiation, cell migration, and gene transcription. Bacterial protein tyrosine phosphatases have structural and sequence similarity to eukaryotic counterparts

but are not as specialized as protein tyrosine phosphatases of eukaryote. β-Nitrostyrene act as phosphotyrosine mimetics, that the nitrovinyl chain was used for Protein Tyrosine Phosphatase 1B (PTP1B) inhibiton by forming a covalent complex with Cys215 at the active site of the protein [4,5,6].

PTP1B, a PTP family member is a major negative regulator of the signal pathway where they are involved [7]. PTP1B consist of 435 amino acid located at the face of the endoplasmic reticulum cytoplasmic, with the molecular weight of 50 kDa and PTP family-owned conservative sequence. The phosphatase catalytic site of PTP1B is localized along the sequence of residues from histidine 214 to arginine 221 in the P fold, in which the critical residues of its active sites are Cys215 and Arg221 [8].

Based on the diversity of PTP1B inhibitory mechanisms, several classes of synthetic compounds and natural products have been characterized for developing as therapeutic agents [9]. Even so, the invention of selective PTP1B inhibitors that possesses good pharmacological aspect is difficult. That's why there are no PTP1B qualified inhibitors found in the clinical trials yet. The basic challenge to find a new inhibitor structure for PTP1B is being identified as phosphotyrosine mimetic having adequate selectivity, very low toxicity and high bioavailability [10]. Fragment based drug design is a new approach in determining the initial chemical starting point for drug discovery projects. The small sized fragments make the following optimization is relatively easier to create the molecule by exploring the chemical cavity in the binding pocket [11]. For that reason, small molecular of PTP1B inhibitors could be promising as candidate drugs for designing the new therapeutic agents of bacterial and fungal infections. Obviously, β-nitrostyrene derivatives can be considered as fragment for the design of the drugs.

Computer-aided docking is a significant tool for achieving understanding about the binding interactions between a ligand and its protein target. This option is a sophisticated tool for drug design, in which small molecules were docked to the known protein structure has become an integral part of the drug discovery process [12]. In the last few years, various virtual screening approach have been developed to predict the some inhibitors activity of PTP1B. Moreover, studies of molecular docking to representative inhibitors are implemented to know the binding poses of inhibitors at the PTP1Bs active site. The result of docking found that studied compounds form hydrogen bonds with some residues such as Arg24, Tyr46, Asp48, Asp181, Ser216, Gly220, Arg221, Arg254, and Gln262 [13, 14].

PTP1B also plays a key role as a negative regulator in signaling pathways of insulin that are involved in type 2 diabetes. The enzyme interacts with insulin receptor as well as substrate-1 of insulin receptor, thereby dephosphorylating phosphotyrosine residues, effecting in down-regulation of insulin action. Type 2 diabetes drives this global pandemic with increasing number of patients over the last decades, accounting for 90% of all cases [9,15]. In addition, PTP1B overexpression has been implicated in the signaling of cancer, tumor and in inflammation processes [16,17,18]. Therefore, PTP1B is also an attractive drug candidate for the therapy of type 2 diabetes and other associated metabolic diseases.

In several previous studies, it was reported that several β-nitrostyrene derivatives were successfully prepared for biological purposes. However, only a few studies related to the bioactivity effect of side chain conformation of the aromatic ring of β-nitrostyrene compounds, especially the type of alkyloxy chain that have not yet been conducted. In the present work, several 3,4-dimethoxy-β-nitrostyrene derivatives were synthesized as antimicrobial agents which correlate with inhibition of PTP1B. In this series, the alkyloxy chain at position 3,4 of β-nitrostyrene is modified. Modifications of substituent at β-carbon of β-nitrostyrene were also carried out to investigate the effect of structural changes on their activity. The antimicrobial activity of an analogous of compounds was assessed and docking simulations of them into the catalytic site of PTP1B were also performed to compare the results.
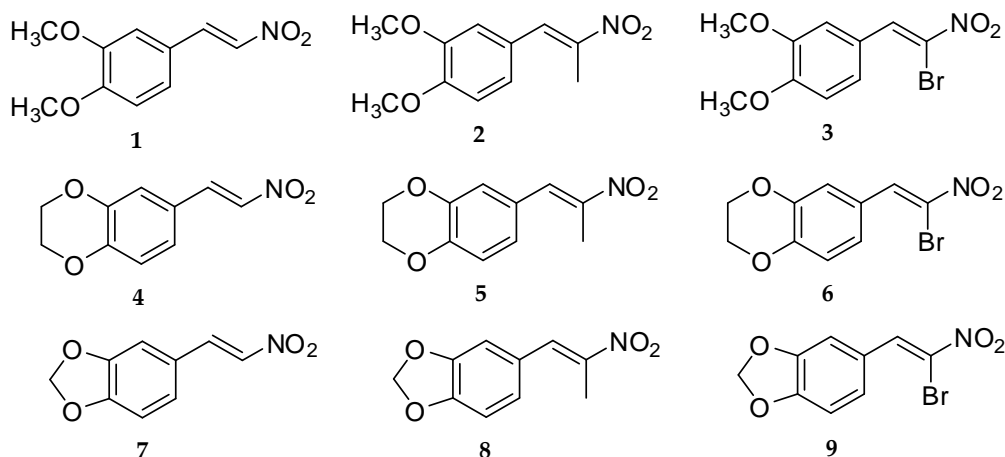
Figure 1. 3,4-Dimethoxy-β-nitrostyrene derivatives synthesized in this research work.

2. Materials and Methods

The major chemicals were obtained from the supplier Sigma-Aldrich (St. Louis, MO, USA). Thin layer chromatography and column chromatography were achieved using Merck 60 F_{254} silica gel and 60 (70-230 mesh) silica gel, respectively (Darmstadt, Germany). FT-IR spectroscopy was done using Bruker ALPHA spectrometer with Ge-ATR (Billerica, MA, USA). ^{1}H- and ^{13}C-NMR analysis was carried out using JEOL JNM ECS-400 spectrometer (Tokyo, Japan) in deuterated chloroform at 400 MHz. Mass spectroscopy was performed on an Agilent 5977B MSD-7890 GC System (Santa Clara, CA, USA). Melting Points were measured using apparatus of Fisher-Johns melting point and are uncorrected. All commercial reagents and solvents used were of analytical grade.

2.1. Synthesis of 3,4-Dimethoxy-β-Nitrostyrene Derivatives

2.1.1. Synthesis of β-Nitrostyrene Series

The slightly modification of Mee *et al* [19] methods, was adapted for the synthesis of the compounds. The corresponding aldehyde was dissolved in stirred glacial acetic acid, ammonium acetate and nitromethane (p = 1.14 g/cm^3) added was then the mixture refluxed and stirred for 2 h at 50 °C (reaction progress monitored by TLC). The dark orange mixture was cooled to room temperature and distilled water was then added. The crude orange product was filtered off, washed with water was then extracted with dichloromethane. The phase of organic were dried over $MgSO_4$, filtered and evaporated under vacuum. The yellow solid was recrystallized twoo times from ethanol to yield the product, melting point determined and identified by spectrometric analysis.

Compound **1**: A mixture of 3,4-dimethoxybenzaldehyde (2.29 g, 14 mmol) and nitromethane (15.96 g, 256 mmol) with ammonium acetate (3.70 g, 48 mmol) in glacial acetic acid (5 ml) was reacted and light yellow crystals were obtained, 1.48 g, 50.5 % yield, mp 139-141 °C. FT-IR (ATR; υ, cm^{-1}): 1491 (asymmetric NO_2), 1358 (symmetric NO_2); ^{1}H NMR (400 MHz, CDCl$_3$): δ$_H$ (ppm): 7.94 (1H, d, J = 13.6 Hz, H-β), 7.52 (1H, d, J = 13.6 Hz, H-α), 7.16 (1H, dd, J = 2.0, 8.0 Hz, H-6), 6.99 (1H, d, J = 2.0 Hz, H-2), 6.89 (1H, d, J = 8.8 Hz, H-5), 3.92 (3H, s, C3-OCH$_3$), 3.91 (3H, s, C4-OCH$_3$); ^{13}C NMR (400 MHz, CDCl$_3$) δ$_C$ (ppm): 152.9 (C-3), 149.6 (C-4), 139.4 (C-α), 135.2 (C-β), 124.7 (C-1), 122.9 (C-6), 111.4 (C-5), 110.3 (C-2), 56.2 (C3-OCH$_3$), 56.1 (C4-OCH$_3$); GC/MS *m/z* (%): 209 (M, 100), 162 (51), 119 (14), 91 (16).

Compound **4**: A mixture of 3,4-ethylenedioxybenzaldehyde (1.29 g, 8 mmol) and nitromethane (9.12 g, 146 mmol) with ammonium acetate (2.11 g, 27.4 mmol) in glacial acetic acid (3 ml) was reacted and light yellow crystals were obtained, 1.20 g, 72.5 % yield, mp 147-149 °C. FT-IR (ATR; υ, cm^{-1}): 1509 (asymmetric NO_2), 1338 (symmetric NO_2); ^{1}H NMR (400 MHz, CDCl$_3$): δ$_H$ (ppm): 7.89 (1H, d, J = 13.2 Hz, H-β), 7.46 (1H, d, J = 13.6 Hz, H-α), 7.06 (1H, d, J = 2.4 Hz, H-2), 7.05 (1H, d, J = 6,8 Hz, H-5), 6.90 (1H, dd, J = 2.4, 6.4 Hz, H-6), 4.33-4.27 (2H, m, C3-OCH$_2$), 4.33-4.27 (2H, m, C4-OCH$_2$);

^{13}C NMR (400 MHz, CDCl$_3$) δ_C (ppm): 147.5 (C-4), 144.1 (C-3), 139.1 (C-α), 135.6 (C-β), 123.6 (C-1), 123.5 (C-6), 118.4 (C-5), 117.9 (C-2), 64.8 (C3-OCH$_2$), 64.2 (C4-OCH$_2$); GC/MS *m/z* (%): 207 (M, 100), 160 (66), 89 (26), 77 (19).

Compound **7**: A mixture of 3,4-methylenedioxybenzaldehyde (1.18 g, 8 mmol) and nitromethane (9.12 g, 146 mmol) with ammonium acetate (2.11 g, 27.4 mmol) in glacial acetic acid (4 ml) was reacted and brownish yellow crystals were obtained, 0.80 g, 52 % yield, mp 158-160 °C. FT-IR (ATR; υ, cm^{-1}): 1492 (asymmetric NO$_2$), 1332 (symmetric NO$_2$); ^{1}H NMR (400 MHz, CDCl$_3$): δ_H (ppm): 7.91 (1H, d, *J* = 13.6 Hz, H-β), 7.46 (1H, d, *J* = 13.6 Hz, H-α), 7.07 (1H, dd, *J* = 1.6, 7.6 Hz, H-6), 6.99 (1H, d, *J* = 1.6 Hz, H-2), 6.86 (1H, d, *J* = 8.0 Hz, H-5), 6.05 (2H, s, C3-OCH$_2$O-C4); ^{13}C NMR (400 MHz, CDCl$_3$) δ_C (ppm): 151.5 (C-3), 148.8 (C-4), 139.2 (C-α), 135.5 (C-β), 126.8 (C-1), 124.2 (C-6), 109.2 (C-2), 107.1 (C-5), 102.2 (C3-OCH$_2$O-C4); GC/MS *m/z* (%): 193 (M, 92), 146 (100), 89 (61), 63 (31).

2.1.2. Synthesis of β-Methyl-β-Nitrostyrene Series

The corresponding aldehyde was dissolved in stirred glacial acetic acid, ammonium acetate and nitroethane (*p* = 1.045 g/cm^3) added was then the mixture refluxed and stirred for 2 h at 50 °C (reaction progress monitored by TLC). The dark orange mixture was then cooled to room temperature then extracted with dichloromethane and washed with distilled water. The layer of organic were dried over MgSO$_4$ then filtered and concentrated under vacuum. The crude orange solid was recrystallized two times from ethanol to yield the product, melting point determined and identified by spectrometric analysis.

Compound **2**: A mixture of 3,4-dimethoxybenzaldehyde (1.66 g, 10 mmol) and nitroethane (14.63 g, 200 mmol) with ammonium acetate (2.71 g, 35 mmol) in glacial acetic acid (5 ml) was reacted and light yellow crystals were obtained, 1.26 g, 56.5 % yield, mp 66-68 °C. FT-IR (ATR; υ, cm^{-1}): 1511 (asymmetric NO$_2$), 1313 (symmetric NO$_2$); ^{1}H NMR (400 MHz, CDCl$_3$): δ_H (ppm): 8.06 (1H, s, H-α), 7.08 (1H, dd, *J* = 2.0, 8.8 Hz, H-6), 6.94 (1H, d, *J* = 2.4 Hz, H-2), 6.93 (1H, d, *J* = 8.4 Hz, H-5), 3.93 (3H, s, C3-OCH$_3$), 3.91 (3H, s, C4-OCH$_3$), 2.48 (3H, s, H-γ); ^{13}C NMR (400 MHz, CDCl$_3$) δ_C (ppm): 150.8 (C-3), 149.1 (C-4), 133.9 (C-α), 145.9 (C-β), 125.1 (C-1), 124.1 (C-6), 113.1 (C-5), 111.3 (C-2), 56.1 (C3-OCH$_3$), 56.1 (C4-OCH$_3$), 14.3 (C-γ); GC/MS *m/z* (%): 223 (M, 100), 176 (51), 131 (25), 91 (16).

Compound **5**: A mixture of 3,4-ethylenedioxybenzaldehyde (0.70 g, 4.3 mmol) and nitroethane (8.36 g, 100 mmol) with ammonium acetate (2.00 g, 26 mmol) in glacial acetic acid (5 ml) was reacted and light yellow crystals were obtained, 0.28 g, 30.3 % yield, mp 73-75 °C. FT-IR (ATR; υ, cm^{-1}): 1503 (asymmetric NO$_2$), 1284 (symmetric NO$_2$); ^{1}H NMR (400 MHz, CDCl$_3$): δ_H (ppm): 7.98 (1H, s, H-α), 6.98 (1H, d, *J* = 2.0 Hz, H-2), 6.96 (1H, dd, *J* = 2.0, 8.4 Hz, H-6), 6.91 (1H, d, *J* = 8.4 Hz, H-5), 4.32-4.27 (2H, m, C3-OCH$_2$), 4.32-4.27 (2H, m, C4-OCH$_2$), 2.44 (3H, s, H-γ); ^{13}C NMR (400 MHz, CDCl$_3$) δ_C (ppm): 146.2 (C-4), 145.5 (C-3), 133.6 (C-α), 143.7 (C-β), 125.7 (C-1), 124.4 (C-6), 119.2 (C-5), 117.9 (C-2), 64.7 (C3-OCH$_2$), 64.3 (C4-OCH$_2$), 14.2 (C-γ); GC/MS *m/z* (%): 221 (M, 100), 174 (78), 103 (38), 91 (29).

Compound **8**: A mixture of 3,4-methylenedioxybenzaldehyde (1.50 g, 10 mmol) and nitroethane (14.63 g, 200 mmol) with ammonium acetate (2.71 g, 35 mmol) in glacial acetic acid (5 ml) was reacted and light yellow crystals were obtained, 0.99 g, 47.6 % yield, mp 88-90 °C. FT-IR (ATR; υ, cm^{-1}): 1508 (asymmetric NO$_2$), 1319 (symmetric NO$_2$); ^{1}H NMR (400 MHz, CDCl$_3$): δ_H(ppm): 8.01 (1H, s,H-α), 6.97 (1H, dd, *J* = 2.0, 8.0 Hz, H-6), 6.93 (1H, d, *J* = 1.2 Hz, H-2), 6.88 (1H, d, *J* = 8.0 Hz, H-5), 6.04 (2H, s, C3-OCH$_2$O-C4), 2.45 (3H, s, H-γ); ^{13}C NMR (400 MHz, CDCl$_3$) δ_C (ppm): 149.4 (C-3), 148.3 (C-4), 133.8 (C-α), 146.2 (C-β), 126.3 (C-1), 126.1 (C-6), 109.6 (C-2), 108.9 (C-5), 101.9 (C3-OCH$_2$O-C4), 14.3 (C-γ); GC/MS *m/z* (%): 207 (M, 83), 160 (87), 103 (100), 77 (43).

2.1.3. Synthesis of β-Bromo-β-Nitrostyrene Series

The corresponding aldehyde was dissolved in stirred glacial acetic acid, ammonium acetate and bromo-nitromethane (*p* = 2.007 g/cm^3) added was then the mixture refluxed and stirred for 2 h at 50 °C (reaction progress monitored by TLC). The dark orange mixture was then cooled to room temperature then extracted with dichloromethane was then washed with distilled water. The

organic extracts were dried over MgSO₄, filtered and concentrated under vacuum. The crude residue was purified using column chromatography over silica gel with eluent of n-hexane-chloroform (1:4) to yield the product, melting point determined and identified by spectrometric analysis.

Compound **3**: A mixture of 3,4-dimethoxybenzaldehyde (0.92 g, 5.5 mmol) and bromo-nitromethane (2.01 g, 12.9 mmol) with ammonium acetate (0.70 g, 9 mmol) in glacial acetic acid (1.5 ml) was reacted and orange crystals were obtained, 0.31 g, 19.6 % yield, mp 110-112 °C. FT-IR (ATR; υ, cm⁻¹): 1517 (asymmetric NO₂), 1307 (symmetric NO₂); ¹H NMR (400 MHz, CDCl₃): δH (ppm): 8.63 (1H, s, H-α), 7.59 (1H, d, *J* = 2.4 Hz, H-2), 7.51 (1H, dd, *J* = 2.0, 8.8 Hz, H-6), 6.96 (1H, d, *J* = 8.8 Hz, H-5), 3.95 (3H, s, C3-OCH₃), 3.93 (3H, s, C4-OCH₃); ¹³C NMR (400 MHz, CDCl₃) δc (ppm): 152.7 (C-3), 149.0 (C-4), 136.7 (C-α), 127.0 (C-1), 125.5 (C-6), 122.7 (C-β), 112.8 (C-5), 111.1 (C-2), 56.2 (C3-OCH₃), 56.1 (C4-OCH₃); GC/MS *m/z* (%): 289 (M, ⁸¹Br, 55), 287 (M, ⁷⁹Br, 56), 162 (100), 147 (45), 91 (29).

Compound **6**: A mixture of 3,4-ethylenedioxybenzaldehyde (0.90 g, 5.5 mmol) and bromo-nitromethane (2.61 g, 17 mmol) with ammonium acetate (0.70 g, 9 mmol) in glacial acetic acid (2 ml) was reacted and light yellow crystals were obtained, 0.90 g, 57.3 % yield, mp 129-131 °C. FT-IR (ATR; υ, cm⁻¹): 1509 (asymmetric NO₂), 1277 (symmetric NO₂); ¹H NMR (400 MHz, CDCl₃): δH (ppm): 8.55 (1H, s, H-α), 7.59 (1H, d, *J* = 1.6 Hz, H-2), 7.39 (1H, dd, *J* = 2.4, 8.8 Hz, H-6), 6.95 (1H, d, *J* = 8.8 Hz, H-5), 4.34-4.28 (2H, m, C3-OCH₂), 4.34-4.28 (2H, m, C4-OCH₂); ¹³C NMR (400 MHz, CDCl₃) δc (ppm): 147.4 (C-4), 143.7 (C-3), 136.3 (C-α), 126.3 (C-β), 125.9 (C-1), 123.3 (C-6), 119.8 (C-5), 117.9 (C-2), 64.8 (C3-OCH₂), 64.2 (C4-OCH₂); GC/MS *m/z* (%): 287 (M, ⁸¹Br, 51), 285 (M, ⁷⁹Br, 53), 160 (100), 104 (45), 76 (35).

Compound **9**: A mixture of 3,4-methylenedioxybenzaldehyde (1.66 g, 11 mmol) and bromo-nitromethane (4.82 g, 30 mmol) with ammonium acetate (1.4 g, 18 mmol) in glacial acetic acid (4 ml) was reacted and brown crystals were obtained, 0.61 g, 20.3 % yield, mp 93-95 °C. FT-IR (ATR; υ, cm⁻¹): 1495 (asymmetric NO₂), 1295 (symmetric NO₂); ¹H NMR (400 MHz, CDCl₃): δH (ppm): 8.58 (1H, s, H-α), 7.62 (1H, d, *J* = 1.6 Hz, H-2), 7.34 (1H, dd, *J* = 1.2, 8.0 Hz, H-6), 6.91 (1H, d, *J* = 8.0 Hz, H-5), 6.08 (2H, s, C3-OCH₂O-C4); ¹³C NMR (400 MHz, CDCl₃) δc (ppm): 151.2 (C-3), 148.3 (C-4), 136.5 (C-α), 129.1 (C-β), 125.8 (C-1), 124.1 (C-6), 109.4 (C-2), 108.9 (C-5), 102.2 (C3-OCH₂O-C4); GC/MS *m/z* (%): 273 (M, ⁸¹Br, 32), 271 (M, ⁷⁹Br, 32), 224 (⁸¹Br, 30), 224 (⁷⁹Br, 30), 146 (100).

2.2. Antimicrobial Assay

The MIC for bacteria, yeast and mold were set in Mueller Hinton Broth at 18 h, 24 h and 5 d, respectively. The strains used for biological tests were: *Staphylococcus aureus*, *Pseudomonas aeruginosa*, *Candida albicans*, and *Aspergillus niger*. Inoculum were prepared by fitting a suspension to match 0.2 optical density (OD) at 600 nm. Broth microdilution testing was adapting to the National Committee for Clinical Laboratory Standards guidelines. The test compounds were prepared in DMSO 2 % at various concentration. Microplate assays for bacterial and yeast were performed in clear using plates of 96-well. The test compounds were applied to the plates containing 100 μL media, with a total volume of 200 μL per well. Microplates were incubated 24 h at 30 °C aerobically before reading wells visually for turbidity. Disk diffusion assay for a mold was performed, a swab dipped into the standardized inoculums were scratched evenly to the plates containing Mueller-Hinton (MH) agar. Suspension disks containing 20 uL of test compounds were added to the surfaces of inoculated plates. Plates were then incubated at 30°C for 5 days to let for fungal growth. The zone diameter of inhibition were measured in millimeters. The positive controls used in this assay are ciprofloxacin for bacteria, nystatin for yeast and griseofulvin for mold. All assays were performed at least twice replicated. MIC results were reported as MIC (μg/mL) for standards. Compounds are evaluated for activity. Statistical analyses were performed using MS Excel 2007.

2.3. Molecular Docking

Molecular docking was conducted using Autodock 4.2 that are supported by Accelrys Discovery Studio 2.1 and Chem3D Ultra 10.0. Visualization of bonding interactions was generated using Chimera 1.13, and Pymol 2.0. The crystal structure of PTP1B (Protein Data Bank, 1XBO) was

extracted from PDB (http://www.rscb.org/pdb). The 1XBO protein contains two chains, A and B, which form a homodimer. Chain A was used for receptor preparation and chain B was the native ligand of 1XBO. The water and native compound molecules were discarded from the crystal pocket, was then polar hydrogens were added to the receptor. The determination of the residues in the active site was used to analyze the Grid box and docking evaluation results. Docking validation was undertaken by analyzing of the root-mean-square deviation (RMSD) between the native ligand structure and the residues in the active site of the protein structure. 3,4-Dimethoxy-β-nitrostyrene derivatives were docked in a flexible manner.

3. Results and Discussion

3.1. Spectroscopy analysis

Spectroscopy analysis indicated that the spectral data obtained from nuclear magnetic resonance and mass spectrometry were compatible with the structures suggested. The NMR and GCMS analysis of the 3,4-dimethoxy-β-nitrostyrene derivatives proposed that the β-E-nitrostyrene conformation was predominant in most of the compounds synthesized. For example, for compound **2** the E/Z ratio is 45/2.

3.2. Antimicrobial Activity

Compound **2** was used for the first assay to investigate the antimicrobial potency of the 3,4-dimethoxy-β-nitrostyrene derivatives by their activity against a strain of bacteria, yeast and a mold. It was also used to choose a microbial strain with the highest activity among them for the further assay. The results view as the minimum inhibitory concentration (MIC) for compound **2** and are displayed in the Tables 1. The second assay was used to evaluate the possible systemic anti-infective agents of the 3,4-dimethoxy-β-nitrostyrenes derivatives as the MIC for each compound and are displayed in the Tables 2.

Table 1. Antimicrobial activity of the compound **2** against several microbial strains.

Strain	Minimum Inhibitory Concentration MIC, (μg/mL)
Staphylococcus aureus	> 128
Pseudomonas auruginosa	> 128
Candida albicans	128
Aspergillus niger	256

The antimicrobial assays shown in Table 1 indicated that compound **2** displayed potential all-round activity. It showed the highest activity against *Candida albicans* (MIC of 128 μg/mL) among the microbial strains. By analyzing the turbidity, compound **2** was also more potent against *Staphylococcus aureus* (gram-positive bacteria) than *Pseudomonas auruginosa* (gram-negative bacteria) (data not show). Table 2 displays the assay results of antimicrobial activity against *Candida albicans* for the 3,4-dimethoxy-β-nitrostyrene analogous under study, with MICs ranging from 32 to 128 μg/mL. Compounds **4** and **7** showed more active than compound **1**. Between compounds **3**, **6**, and **9**, **6** was the most active compound against *Candida albicans*, also between compounds **2**, **5**, and **8**, **5** was clearly superior. Therefore, the ethylenedioxy grup in position 3,4- of benzene ring gave more inhibitory effect than the methylenedioxy or dimethoxy grups. The 3,4-dimethoxy series was the weakest agents, they gave almost identical results in activity against *Candida albicans*. Among 3,4-ethylenedioxy series, **4** and **5** were more effective but there is little difference in their activity. Between Compounds **7**, **8**, and **9**, **7** was the most active compound against *Candida albicans*. So that,

the grup of a β-methyl or a β-bromine at nitrovinyl chain induces to a decrease of the inhibitory effect. However, the fact that **5** is better than **6** indicates that in this case, β-methyl substitution leads to higher activity than β-bromo substitution. In addition, previously there have been several antibacterial assays on compounds **1**, **2**, **7** and **8** against several strains with different MIC values [3,4,5,6].

Table 2. Antimicrobial activity of the 3,4-dimethoxy-β-nitrostyrene derivatives against *Candida albicans*.

Compound	Minimum Inhibitory Concentration MIC, (μg/mL)
1	128
2	128
3	128
4	32
5	32
6	64
7	32
8	128
9	128

The greater activity of some 3,4-dimethoxy-β-nitrostyrene derivatives might indicate that they act as tyrosine mimetics, interacting tyrosine phosphatases (PTP) and interrupting with cell signaling in strains. Tyrosine phosphorylation in eukaryotes such as *Candida albicans* controls cell differentiation, cell migration, and gene transcription. These enzymes are involved in other cellular processes, such as cell wall synthesis, formation of hyphae and maintenance of cellular integrity in stress situations. Tyrosine phosphorylation also known are involved in mitogen-activated protein (MAP) kinase signaling cascades. The MAP kinase cascade in *Candida albicans* can trigger the transition of the budding yeast to form a more invasive filamentous yeast [4, 20, 21].

Park and Pei have proposed that the PTPs was a Protein tyrosine phosphatase 1B (PTP1B). They also argued that β-nitrostyrene compounds inhibited PTP1B by their interaction and formation of a covalent complex with Cys215 residue at the active site [4]. In order to find out more about the interaction of 3,4-dimethoxy-β-nitrostyrene derivatives on their binding pocket of PTP1B, a molecular docking with corformational analysis was carried out.

3.3. Molecular Docking

Docking validation was performed to gain the best geometry of ligand-protein by re-docking the original ligand to the receptor. The best result of the RMSD analyzing between the native ligand structures and the residues of the receptor active site is 1.36 Å. The interaction between them is displayed in Figure 2.
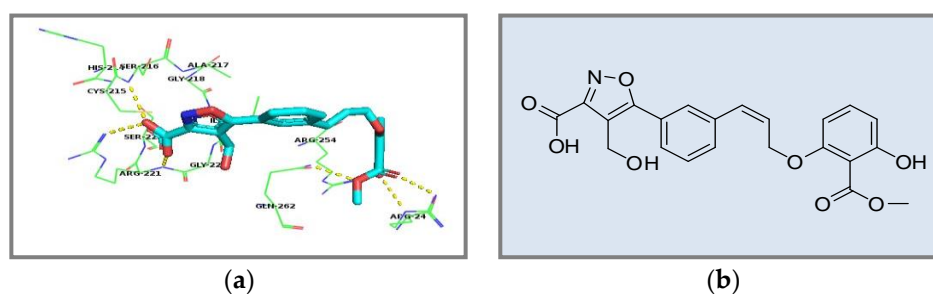

(a)   (b)

Figure 2. (a) The PTP1B (1XBO) amino acid residues around orginal ligand; (b) the native ligand structure.

The results of docking analysis (Table 3) showed that 3,4-dimethoxy-β-nitrostyrene derivatives form H-bonds with the 1XBO amino acids Ser216 and Arg221 and they were surrounded by residues in the active site of 1XBO (Figure 3).

Table 3. Binding energies calculated for the compounds using Autodock 4.2.

Compound	Binding Energy (kcal/mol)	Inhibition Constant	Hidrogen Bonding interacting residues
Native ligand	-10.35	25.78 nM	Arg24, Ser216, Arg221, Arg254, Gly262
1	-7.61	2.63 µM	Ser216, Arg221
2	-8.04	1.28 µM	Ser216, Arg221
3	-8.26	887.98 nM	Ser216, Arg221
4	-7.92	1.57 µM	Ser216, Arg221
5	-8.32	799.81 nM	Ser216, Arg221
6	-8.51	577.04 nM	Ser216, Arg221
7	-7.62	2.62 µM	Ser216, Arg221
8	-7.97	1.45 µM	Ser216, Arg221
9	-8.29	840.19 nM	Ser216, Arg221
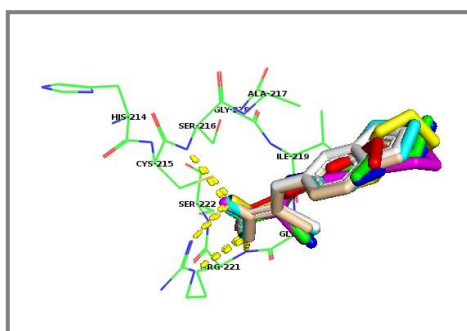
Figure 3. Molecular docking related PTP1B inhibition by 3,4-dimethoxy-β-nitrostyrene derivatives. Binding sites of compounds **1**, **2**, **3**, **4**, **5**, **6**, **7**, **8**, and **9** are represented by red, green, blue, yellow, magenta, cyan, orange, tint, and gray structures, respectively. The figure was generated using PyMol 2.0.

This result was consistent with the inhibition activities of the all compounds. The binding energies obtained from docking 1XBO with 3,4-dimethoxy-β-nitrostyrene derivatives, which compound **6,** the new synthesized compound was the best docking structure with the binding energy of -8,51 kcal/mol, the lowest energy among the series. The detailed binding site of compound **6** is displayed in Figure 4**.** Four H-bonds were formed by compound **6** with Arg221, while only one H-bond was formed with Gly216. The nitro group of compound **6** binds to the Arg221 residue via hydrogen bonding interactions involving α-NH$_2$, δ-NH, δ-NH and ω-NH$_2$ with the bond distances of 1.952, 1.849, 2.387 and 1.621 Å, respectively. It also forms an H-bond with Gly216 residue involving α-NH$_2$ and bond distances of 1.782 Å. To compare the inhibitory ability of compound **6**, phosphorilated tyrosine which acts as substrate of PTP1B in the living system was also docked where the docking result is displayed in Figure 5. The binding energy and inhibition constant of the substrate were -8.34 kcal/mol and 772.7 nM, respectively. It forms H-bonds with the 1XBO amino acids Ser216, Ala217, Gly220 and Arg221.
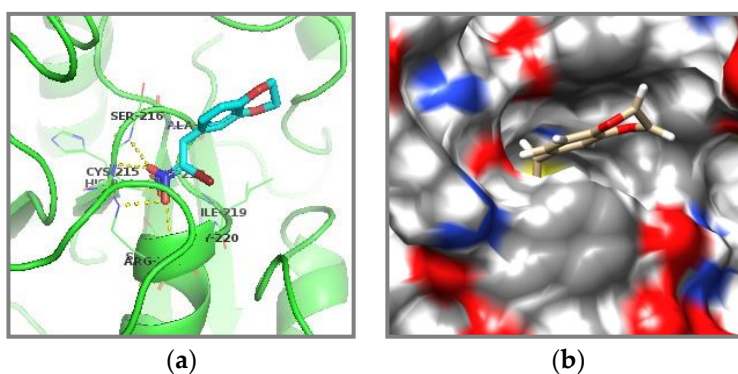
Figure 4. Docking result of compound **6** in the PTP1B catalytic site. (a) Key residues surrounding **6**; (b) Binding pose of **6**.
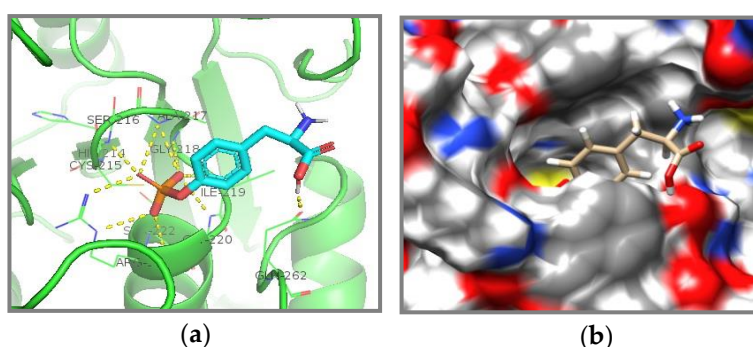

Figure 5. Docking result of phosphorilated tyrosine in the PTP1B catalytic site (a) Key residues; (b) Binding pose.

The result of docking showed that all compounds are surrounded by residues in the active site of 1XBO (214-221 residues), in which the critical of catalytic sites are Cys215 and Arg221 [5]. They showed interaction with Arg221 residue, while there is none with Cys215 residue. The Interaction between a molecule with Cys215 residue can occur via Michael addition in which sulfhydryl groups of cysteine act as attractive nucleophiles to the conjugated nitroalkene as acceptor [5]. This will occur if the distance between the sulphur of Cys215 and the α-carbon of 3,4-dimethoxy-β-nitrostyrene derivatives is suitable for making C-S bonds (<1.82 Å) [22, 23]. The bond distances between them were determined using pymol 2.0 and the result is displayed in Table 4, which it is still relatively far. Therefore, the compounds may not be able to interact with the Cys215. Even so, the α-carbon of compound **2** was the closest with the sulphur of Cys215, shown in Figure 6.

Table 4. The bond distance between α-carbon of all compounds and the sulphur of Cys215 calculated using pymol 2.0.

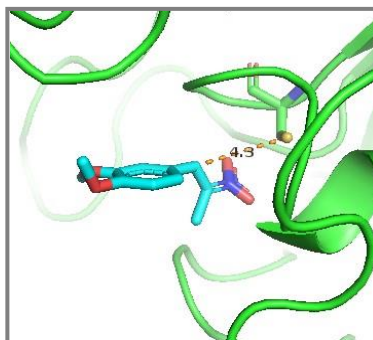| Compound	Bond Distance (Å)
1	4.8
2	4.3
3	4.4
4	4.7
5	4.5
6	4.9
7	4.8
8	5.0
9	5.0

Figure 6. The bond distance between β-carbon of compound **2** and thiol of Cys215 simulated using pymol 2.0.

The result of conformational analysis showed that side chain of aromatic ring and substituent of β-carbon of β-nitrostyrene chain affect the direction of the nitro group to be in the appropriate position to bind with hydrogens. Molecular conformation before and after molecular docking, which are in the most stable geometries is displayed in figure 7. The change in direction of the the nitro group relative to the benzene were investigated by determination of the dihedral angle between their plane, which are relatively greater based on the order of the substituent in β-carbon: H < CH$_3$ < Br (Table 5). Of course, it corresponds to binding energy. The magnitude of the angle was calculated from the dihedral angles of C$_6$-C$_1$-C$_\alpha$-C$_\beta$ and C$_\alpha$-C$_\beta$-N-O.

Table 5. The dihedral angle of the nitro gup relative to the benzene calculated office using Chem3D Ultra 10.0.

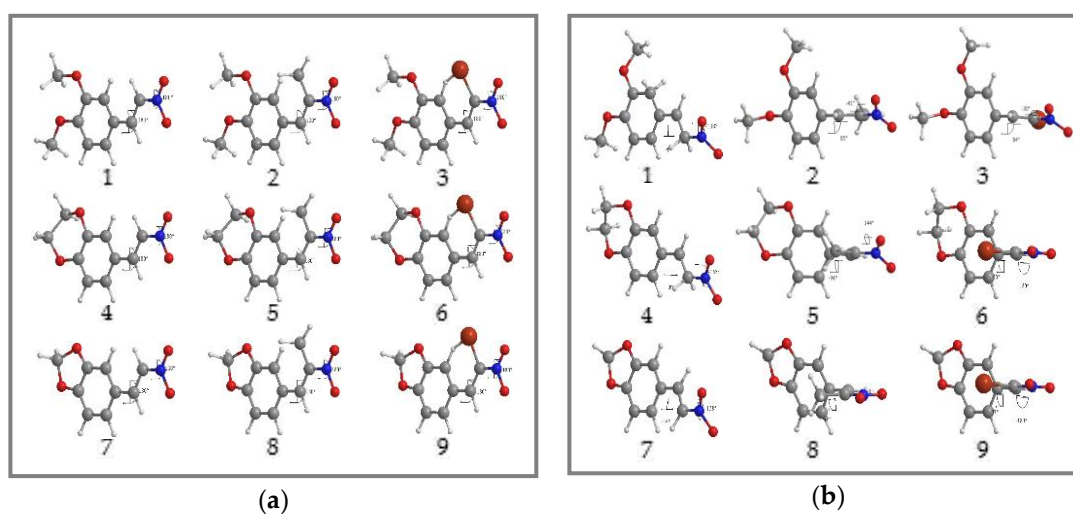| Compound	Angle (°)
1	38
2	44
3	54
4	17
5	48
6	87
7	28
8	82
9	83

Figure 7. (a) The conformation for each compound in the most stable geometries before molecular docking; (b) After molecular docking.

However, the binding energies of all compound were negative (ranging from -7.61 to -8.51 kcal/mol) indicating that the existence of hydrogen bonds might stabilize the open shape of the enzyme and supply tighter binding to the PTP1B active site, so that inhibition of PTP1B becomes more effective. In general, the ethylenedioxy grup in position 3,4 of benzene ring relatively gave more inhibitory effect than the methylenedioxy or methoxy grups. The results of this docking study support the results of antimicrobial activity against *Candida albicans*. It is possible to propose that compound **5** with MIC of 32 mg/L and Binding energy of -8.32 kcal/mol is the best candidate of PTP1B inhibitor as like as antimicrobial agent. However, further study is required in order to prove this argument.

4. Conclusions

The 3,4-dmethoxy β-nitrostyrene derivatives exhibited as potential antimicrobial activity especially against *Candida albicans*. Modification of the alkyloxy side chain at 3,4 position of the aromatic ring significantly influences the antifungal activity of β-nitrostyrenes which is relatively in accordance with the docking result as a PTP1B inhibitor. The 3,4-ethylenedioxy series showed the best activity of the 3,4-dimethoxy-β-nitrostyrene derivatives. Therefore, an extended set of substituted 3,4-ethylenedioxy-β-nitrostyrene compounds will be explored to determine the structural frame desired for the enhancement antimicrobial activity and PTP1B inhibitor. Changes in the nitrovinyl chain of the series can also be undertaken, specifically in the volume and length of its substituents, in order to investigate its distance to Cys215 of PTP1B which supports Michael addition. Further *in vivo* works to elucidate the effects and toxicity of these derivatives are needed.

Conflicts of Interest: The authors declare no conflict of interest.

References

1. Shapiro, R.S.; Robbins, N.; Cowen, L.E. Regulatory circuitry governing fungal development, drug resistance, and disease. *Microbiol. Mol. Biol. Rev*. **2011**, *75*, 213-267.
2. Khabnadideh, S.; Rezaei, Z.; Pakshir, K.; Zomorodian, K.; Ghafari, N. Synthesis and antifungal activity of benzimidazole, benzotriazole and aminothiazole derivatives. *Res. Pharm. Sci*. **2012**, *7*, 65-72.
3. Milhazes, N.; Calheiros, R.; Marques, M.P.M.; Garrido, J.; Cordeiro, M.N.D.S.; Rodrigues, C.; Quinteira, S.; Novais, C.; Peixe, L.; Borges, F. β-Nitrostyrene derivatives as potential antibacterial agents: A structure-property-activity relationship study. *Bioorg. Med. Chem.* **2006**, *14*, 4078-4088.
4. Nicoletti, G.; Cornell, H.; Hügel, H.M.; White, K.S.; Nguyen, T.; Zalisniak, L.; Nugegoda, D. Synthesis and antimicrobial activity of nitroalkenylarenes. *Anti-Infective Agents* **2013**, *11*, 179-191.
5. Cornell, H.; Nguyen, T.; Nicoletti, G.; Jackson, N.; Hügel, H.M. Comparison of halogenated β-nitrostyrene as antimicrobial agents. *Appl. Sci.* **2014**, *4*, 380-389.
6. Lo, K.; Cornell, H.; Nicoletti, G.; Jackson, N.; Hügel, H.M. A study of fluorinated β-nitrostyrene as antimicrobial agents. *Appl. Sci.* **2012**, *2*, 114-128.
7. Tonks, N.K. PTP1B: From the sidelines to the front lines!. *FEBS Letters* **2003**, *546*, 140-148.
8. Sun, J.; Qu, C.; Wang, Y.; Huang, H.; Zhang, M.; Li, H.; Zhang, Y.; Wang, Y.; Zou, W. PTP1B, a potential target of type 2 diabetes mellitus. *Mol. Biol.* **2016**, *5*, 174.
9. Tamrakar, A.K.; Maurya, C.K.; Rai, A.K. PTP1B inhibitor for type 2 diabetes treatment: a patent reiview (2011 – 2014). *Expert Opin. Ther. Patents.* **2014**, *24*, 1-15.
10. Verma, M.; Gupta, S.J.; Chaudhary, A.; Garg, V.K. Protein tyrosine phosphatase 1B as antidiabetic agents - a brief review. *Bioorganic Chemistry* **2017**, *70*, 267-283.

11. Reddy, M.V.V.V.S.; Chakshusmathi, G.; Narasu, M.L. Small molecule inhibitors of PTP1B and TCPTP. *Int. J. Pharm. Phytopharmacol. Res.* **2012**, *1*, 287-291.

12. Rizvi, S.M.D.; Shakil, S.; Haneef, M. A simple click by click protocol to perform docking: Autodock 4.2 made easy for non-bioinformaticians. *EXCLI Journal* **2013**, *12*, 831-857.

13. Wang, F.; Zhou, B. Toward the identification of a reliable 3D-QSAR model for the protein tyrosine phosphatase 1B inhibitors. *Journal of Molecular Structure* **2018**, *1158*, 75-87.

14. Ali, M.Y.; Kim, D.H.; Seong, S.H.; Kim, H.; Jung, H.A.; Choi, J.S. α-Glucosidase and protein tyrosine phosphatase 1B inhibitory activity of plastoquinones from marine brown alga *Sargassum serratifolium*. *Mar. Drugs.* **2017**, *15*, 368.

15. Sotiriou, A. Novel Target for The Development of drug for Type 2 Diabetes Mellitus. Ph.D. Thesis, Wageningen University, Wageningen, Netherland, Desember 2016.

16. Na, B.; Nguyen, P.H.; Zhao, B.T.; Vo, Q.H.; Min, B.S.; Wo, M.H. Protein tyrosine phosphatase 1B (PTP1B) inhibitory activity and glucosidase inhibitory activity of compounds isolated from *Agrimonia pilosa*. *Pharm. Biol.* **2015**, *54*, 474-480.

17. An, J.P.; Nguyen, P.H.; Ha, T.K.Q.; Kim, J.; Cho, T.O.; Oh, W.K. Protein tyrosine phosphatase 1B from the stem of *Akebia quinata*. *Molecules* **2016**, *21*, 1091.

18. Wiese, J.; Aldemir, H.; Schmaljohann, R.; Gulde, T.A.M.; Imhoff, J.F. Asparentin B, a new inhibitor of Protein tyrosine phosphatase 1B. *Mar. Drugs.* **2017**, *15*, 191.

19. Mee, S.P.H.; Baldwin, J.E.; Cowley, A. Total synthesis of 5,5',66'-tetrahydroxy-3,3'-biindolyl, the proposed structure of a potent antioxidant found in Beetroot (*Beta vulgaris*). *Tetrahedron* **2004**, *60*, 3695-3712.

20. Mesquita, A.L.F.; Fernandes, J.R.M. Biochemical Properties and Possible Roles of Ectophosphatase Activities in Fungi. *Int. J. Mol. Sci.* **2014**, *15*, 2289-2304.

21. Csank, C.; Makris, C.; Meloche, S.; Schröppel, K.; Rölinghoff, M.; Dignard, D.; Thomas, D.Y.; Whiteway, M. Derepressed hyphal growth and reduced virulence in a VH1 family-related protein phosphatase mutant of the human pathogen *Candida albicans*. *Molecular Biology of the Cell* **1997**, *8*, 2539-2551.

22. Downard, K.M.; Sheldon, J.C.; Bowie, J.H.; Lewis, D.E.; Hayes, R.N. Are the elusive ions mercaptomethyl ($-CH_2SH$), hydroxymethyl ($-CH_2OH$), and aminomethyl ($-CH_2NH_2$) detectable in the gas phase? A joint ab initio/experimental approach. *J. Am. Chem. Soc.* **1989**, *111*, 8112-8115.

23. Trinajstić, N. Calculation of carbon-sulphur bond lengths. *Tetrahedron Letters* **1968**, *9*, 1529-1532.